Journal of Engineering and Technology Research

Volume 6 Number 2 March 2014

ISSN 2006 - 9790

Academic Journals

ABOUT JETR

The **Journal of Engineering and Technology Research (JETR)** is published monthly (one volume per year) by Academic Journals.

Journal of Engineering and Technology Research (JETR) is an open access journal that provides rapid publication (monthly) of articles in all areas of the subject such as Artificial Intelligence Applications and Innovations, Information Systems, Kinetic Processes in Materials, strength of building materials, engineering applications for world problems etc.
The Journal welcomes the submission of manuscripts that meet the general criteria of significance and scientific excellence. Papers will be published shortly after acceptance. All articles published in JETR are peer-reviewed.

Contact Us

Editorial Office: jetr@academicjournals.org

Help Desk: helpdesk@academicjournals.org

Website: http://www.academicjournals.org/journal/JETR

Submit manuscript online http://ms.academicjournals.me/

Editorial Board

Journal of Engineering and Technology Research

Table of Content: Volume 6 Number 2 February 2014

ARTICLES

Research Articles

academicJournals

Vol. 6(2), pp. 13-17, March 2014
DOI: 10.5897/JETR2014.0352
Article Number: DA4B34C46991
ISSN 2006-9790

http://www.academicjournals.org/JETR

Journal of Engineering and Technology Research

Full Length Research Paper

Investigation of self-similar nature of video streaming traffic in corporate network

Shalangwa D. A.[1]* and Malgwi D. I.[2]

[1]Department of Physics, Adamawa State University, Mubi, Adamawa State, Nigeria.
[2]Department of Physics, University of Maiduguri, Borno State, Nigeria.

Received 20 January, 2014; Accepted 4 February, 2014

In this work, a model of the corporate network had been developed, simulated and implemented using an optimized network engineering tool in a simulation area of 1.5 × 1.5 km enterprise topology network to stream video between each other. Total of 14,670 video traffic (traffic load) is streamed from different sources and destinations at random. The video streaming traffic is monitored, analyzed in view of identifying traffic self-similarity in the network. The results of the analysis show that video traffic is highly self-similar in the network using Abry-Veitch and smoothing algorithms method. The effect of self-similarity in the network is reduced with the help of 1D wavelet technique.

Key words: Smoothing algorithms, video, traffic, optimized network engineering tools (OPNET), self-similar.

INTRODUCTION

Today, the increasing demand in telecommunication service make the structure of network traffic very complex more especially with the introduction of multimedia service such as audio and video streaming over IP network in addition to the traditional web browsing, file transfer protocol, email and so on. Due these massive demands it is then predicted that traffic in most telecommunication network becomes inherently self-similar in nature. Traffic monitoring is a very difficult task because one would not know exactly when input characteristics will change (Karagiannis et al., 2002). Unfortunately they are limited mathematical model to capture the traffic behavior while traffic volume continuous to grow in its exponential form.

When we want to study traffic of all kinds in telecommunication network usually question of constructing a model of input characteristics (volume of the traffic) arises. However, to design a suitable model for any network and to develop fast algorithms of free flow of information across a network from source to destination, understanding network traffic become a critical issue because the fundamental aim of network monitoring is to deliver an outstanding quality of service to the end user with little or no interference.

Many researches in this field show that in general, telecommunication traffic are self-similar or fractal in nature (Adas, 1997; Chaoming, 2005; John, 1981; Oleg et al., 2007; Nikolai, 1995; Nagurney, 2008; Walter, 1997) been global system for mobile communication [GSM], GPRS or Ethernet. The presence of self-similarity in a network may be associated with amplified queing delay, packet loss rate, bottle neck or affect buffer capability (Beryes, 2007; Hamibindu et al., 2007).

In order to investigate the presence of self-similarity in our developed simulated network model, we imposed high-resolution video traffic statistics and we monitored video streaming traffic for several minutes. The behavior of internet traffic is usually time dependent and they are

*Corresponding author. E-mail: deshalangs3g@yahoo.com.

Table 1. Simulation metrice parameter.

Simulation size	1.5 × 1.5 km
Traffic monitored	Video
Simulation time	30 min
Application configuration setting	High-resolution Video
2 LANs	3 host users each

Table 2. Sample statistics of all the observations for video streaming.

		Sample mean(s)	Min value(s)	Max value(s)	Range
All Observations	1 4,670	145.25	0	121	121

usually considered being long range dependence (LRD) while self-similar behavior of network traffic is best described in terms of long range dependence and autocorrelation function of the time series (Guaghui et al., 2004; Karagiannis et al., 2002).

There are various popular methods in which self-similar nature of internet traffic can be identified for example using time-variable plot, periodogram, ratio variance residuals, wavelet, absolute moment, whittle, and R/S method. While in this work we used two techniques to check the presence of self-similarity in our simulated network model. That is log plot of Abry-Veitch and smoothing algorithms while in second method we closely observed the autocorrelation function (ACF) and fast Fourier transform energy spectrum behavior to validate our results.

This work considers two separate corporate networks located at a remote locations to each other with at least three host users in each corporate network streaming video to one another.

IMPLEMENTATION OF THE SIMULATION MODEL

An optimized network engineering tools (OPNET) is used to realize the entire structure of the network in a simulation area of 1.5 km × 1.5 km enterprise topology network. The simulation model is first created using a startup wizard. The topology of each corporate network is then created. The required number of the nodes is dragged into the empty space base on number of nodes required per corporate network, then the nodes fields are adjusted as follows to enable them stream video to each other. The application configuration attribute is set to video to enable us stream video across the network, profile configuration attribute is also set to match with application configuration attribute while the personal computer attributes at each corporate network are set to support the profile as given in the simulation matrices parameter of Table 1.

Collection of statistics

In OPNET, there are two major statistics available that is global statistics and nodes statistics; global statistics tell us about the statistics of the entire network while node statistics tell us about the statistics of an individual node. Appropriate statistics are then imposed on the model. Simulation is run, and the result is taking.

Mathematical relationship between LRD and self-similarity

If we assume X (t) is a second order stochastic stationary process. Let's consider β(x), ρ(x) be the ACF and spectrum of the second order stochastic stationary process. There is a close relationship that exist between LRD and self-similarity given by:

$\beta = 2H - 1$ when $\frac{1}{2}$ <H<1 is valid

$\beta x(p) \sim k_{\beta} |p|^{-\infty}$ as $|p|$ $where \infty \in (0,1)$

$\rho x(q) \sim k_{\rho} |q|^{-|1-\infty|}$ as $|q|$ $where \infty \in (0,1)$

$\beta x(p)$ Usually goes to zero slowly called LRD;

If Z(t) is said to be self-similar If and only if $k^{-H} Z(kt) = Z(t)$, $when\ k$ >0

RESULTS AND DISCUSSION

The result given in Table 2, is video streaming for the length of simulation assumed to be the same with video streaming data traffic in real life network as shown in Figure 1 shows the video streamed data traffic for the length of the simulation, on the vertical axis is the video traffic sent in packet per second against time in second on the horizontal axis. It seems that slightly close to 60 s no packet is transmitted thereafter the video packets were transmitted continuously with an increase in packets, slightly above 60 s, the packets exhibit stochastic stationary behavior. Stochastic stationary process is one of condition of suspecting self-similarity in a network (Higuchin, 1988). Figure 2 present log plot of the video data traffic; for the process to be LRD the logscale plot will exhibit a region where by the log scale plot will be approximately linear with time axis while remain constant with the video traffic axis then the H

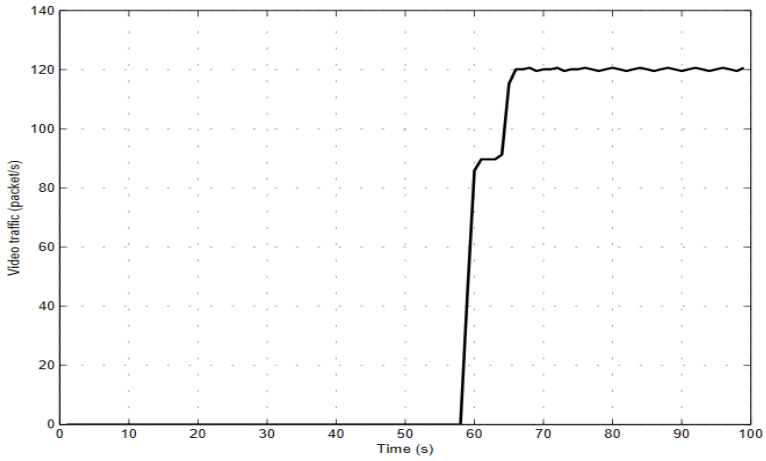

Figure 1. Video streamed data traffic.

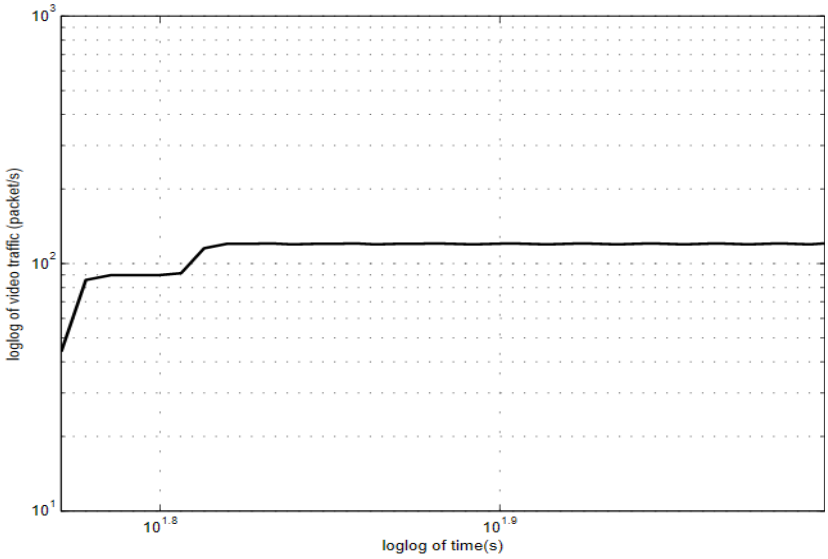

Figure 2. Loglog plot of video data traffic streamed.

exponent can be estimated from logscale plot by {H=(slope+1)/2} (Abry et al., 1998). The slope is calculated as 14.32 while the Hurst exponent is evaluated as 7.66; this evident that in this work video data traffic is highly self-similar considering the fact that for traffic in the network to become self-similar Hurst exponent must falls within 0.5<H<1; the degree of the self-similarity increases as H get close to 1 (Oleg et al., 2007).

In the second method, we used smoothing algorithms. Smoothing algorithms has shown sufficient performance over different sets of data (Umer et al., 2008). Having known that the process is stochastic stationary, we then apply the smoothing algorithms technique; this technique involve different decomposition and reconstruction levels of a signal (video data traffic) using 1D wavelet (Rami, 2011) also taking into consideration ACF which is believed, that its coefficient decay slowly to zero with LRD which describe the intensity of self-similarity in network (Karim, 2007). Next we decomposed, de-noised and reconstructed the stochastic stationary video data traffic step by step up to 5 levels using db 10 wavelet type to validate the ACF and FFT energy spectrum property as given in Figure 3 to 5. When a process is decomposed and reconstructed up to 5 levels it means the process is highly LRD because the maximum decomposition and reconstruction level of db wavelet type is 7; the higher the level of the decomposition and reconstruction stronger the LRD as well as self-similarity (Xiaomo et al., 2004).

In Figure 3 the ACF coefficient is almost zero, FFT has less energy indicating strong relationship with LRD, Figure 4, ACF coefficient move slightly from zero. FFT energy increases showing a decrease in relationship with LRD while Figure 5, ACF coefficient increase significantly,

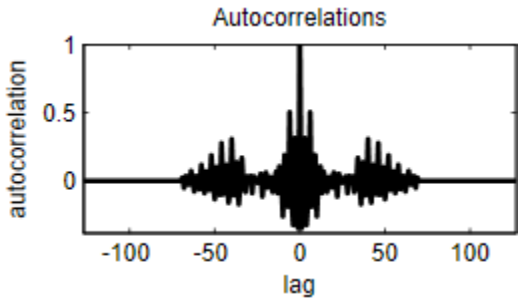

Figure 3a. ACF after level 1 reconstruction.

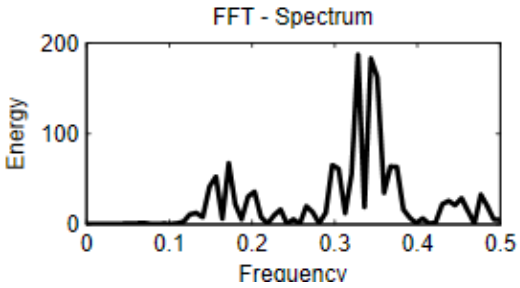

Figure 3b. FFT after level 1 reconstruction.

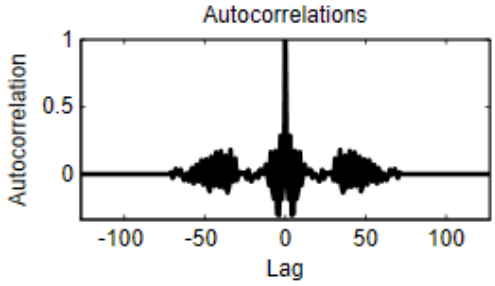

Figure 4a. ACF after level 3 reconstruction.

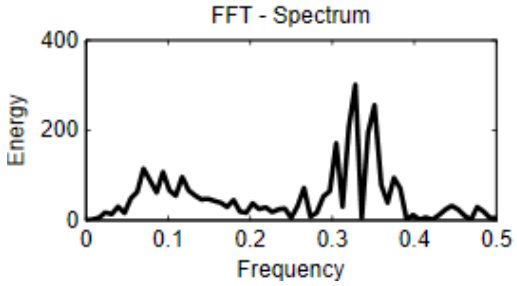

Figure 4b. FFT after level 3 reconstruction.

FFT energy increase tremendously showing poor relationship with LRD as well as self-similarity. Figure 6 present the original data traffic and de-noised data traffic assuming the LRD and self-similarity are not applicable

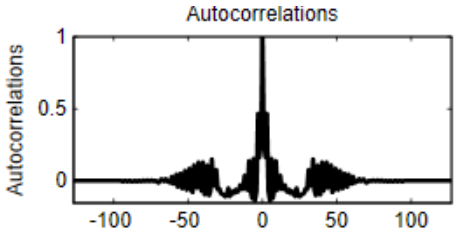

Figure 5a. ACF after level 5 reconstruction.

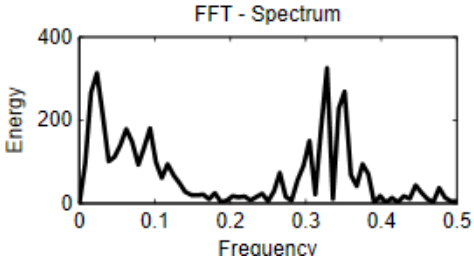

Figure 5b. FFT after level 5 reconstruction.

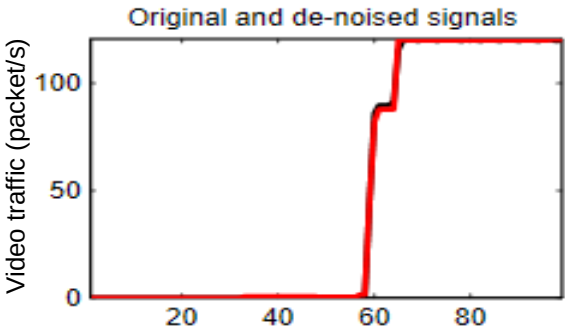

Figure 6. Original and de-noised video traffic data.

to the network. Therefore, it is expected that minimal delay, packet loss, packet retransmission and high buffer capacity will be the feature of the simulated network.

Conclusion

A video traffic had been monitored, analyzed in a model of simulated network developed with a view of checking presence of self-similarity in the network using Abry-Veitch and smoothing algorithms method. Both methods revealed that video traffic is highly LRD and self-similar. The presences of self-similarity in any telecommunication network change the characteristics or behavior of the network by affecting the overall network quality of service (QoS). This work is centered on checking and reducing self-similar properties of network, but does not take into

consideration the causes of self-similarity in the network. Hope this work has provided some basic information on how to investigate self-similarity of video traffic in telecommunication network and reduce its effects. Further recommends that another research work should be conducted to identify the causes of the self-similar process in telecommunication network.

Conflict of Interests

The author(s) have not declared any conflict of interests.

REFERENCES

Abry P, Veitch D (1998). Wavelet analysis of long range dependence traffic. IEEE Trans. Inf. Theory 44(1):2-15. http://dx.doi.org/10.1109/18.650984

Adas A (1997). Traffic models in broadband network. IEEE Communication Magazine. http://dx.doi.org/10.1109/35.601746

Beyers D (2007). Packet radio network research, development and application.Proceeding SHAPE Conference on packet radio, Amsterdam.

Chaoming S, Shlomo H, Hernan AM (2005). Self-Similarity of complex network. Nature. 433:392. http://dx.doi.org/10.1038/nature03248

Hamibindu P, Ying Z, Morley ZM, Charlie YH (2007). Understanding network delay changes by routing events. Proceeding of ACM SIGMETRICS.

Higuchin T (1988). Approach to an irregular time series on the basis of the fractal theory. Physica B. 30:277-283. http://www.sciencedirect.com/science/article/pii/0167278988900814

John EH (1981). Fractal and self-similarity. J. Math. Univ. Indiana 30(5):713-747. http://dx.doi.org/10.1512/iumj.1981.30.30055

Karagiannis T, Faloutsos M, Riedi RH (2002). Long range dependence: Now you see it, now you don't. IEEE Global Internet.

Karim MR (2007). Identifying long range dependence of network traffic through autocorrelation function. Proceeding of 32nd Annual Conference on Local Computer Network pp. 15-18.

Nagurney A, Qiang Q (2007). A Network efficiency measure for congested network. Europhys. Lett. 79(38005):1-5. http://supernet.isenberg.umass.edu/articles/nagurney-epl_final.pdf

Nikolai L, Boris T (1995). An analysis of an ATM buffer with self-similarity (fractal) input traffic 14th Annual IEEE Conference. http://www.psu.edu/

Oleg IS, Sergey MS, Andrey VO (2007). Self-similar process in Telecommunications. John Wiley and Sons, Ltd.

Rami C (2011). Signal denoising using wavelets. Project report. http://tx.technion.ac.il/~rc/SignalDenoisingUsingWavelets_RamiCohen.pdf

Umer H, Mohammed SA (2008). Statistical properties of white. LUMS School of Science Engineering.

Walter W, Murad ST, Robert S, Daniel VW (1997). Self-Similarity through high-variability: Statistical analysis of Ethernet LAN traffic at the source level. IEEE Trans. 5(1):71-86.

Xiaomo J, Hojjat A (2004). Wavelet packet autocorrelation method for traffic flow pattern analysis. Computer Aided Civil Inf. Eng. 19:327-337.

academicJournals

Vol. 6(2), pp. 18-26, March 2014
DOI: 10.5897/JETR2014.0353
Article Number: 2BE3B1446993
ISSN 2006-9790

http://www.academicjournals.org/JETR

Journal of Engineering and Technology Research

Full Length Research Paper

Effect of Argon plasma and ion beam on the morphology and wettability of polyethylene terephthalate (PET)

A. Atta[1], A. M. Abdel Reheem[2] and M. M. Abdel Rahman[2]*

[1]Physics Department, National Center for Radiation Research and Technology (NCRRT), Atomic Energy Authority (AEA), Cairo Egypt.
[2]Accelerators and Ion Sources Department, Nuclear Research Center, Atomic Energy Authority, P. O. Box 13759 Inchas, Cairo, Egypt.

Received 27 January, 2014: Accepted 6 March, 2014

Plasma and ion beams are considered tools that can improve existing materials or create new materials. Their technology is widely used to alter the surface properties of polymers without affecting their bulk properties. The treated polymers have found various applications in microelectronics, biomedical and chemical industries. In this work, the use of Argon plasma and Argon ions produced from cold cathode ion source as a method for the morphology and wettability of Semi crystalline polyethylene terephtalate (PET) foils are investigated. A cold cathode ion source was used as a preparation tool of the surface of polyethylene terephthalate PET polymer substrate to be ready for various applications as coating or thin film deposition. Argon ions of 1.5 keV are produced from the cold cathode ion source with an operating gas pressure of 2×10^{-4} mbar. The induced effects in the structure, surface morphology, and surface wettability were investigated by means of the Fourier transform infrared spectroscopy (FTIR), scanning electron microscope (SEM) and by the contact angle methods, respectively. The change in the contact angle on PET as a function of Argon plasma time and ion beam fluence was also studied. Changes in surface free energy of polymer surface after Argon plasma irradiation were observed.

Key words: Cold cathode ion source, Argon plasma and ion beams, polyethylene terephthalate (PET) foils.

INTRODUCTION

Polymer materials with improved mechanical, optical or electrical properties have been widely used in a variety of industrial applications. However, their use is sometimes limited by undesired properties of the surface, contrary to very useful characteristics of the bulk, such as low weight, chemical inertness and high impact resistance. Therefore, it is interesting to modify the surface in a controlled manner to enhance wettability, printability, adhesion with other materials or with biological components, compatibility (as in the production of

*Corresponding author. E-mail: moustafa82003@yahoo.com.

material blends using two immiscible polymers), etc. (Cho et al., 2003; Ektessabi and Sano, 2000; Spohr, 1990; Ektessabi and Yamaguchi, 2000). Plasma treatment does not produce toxic waste in contrast to the treatments using chemicals. The plasma is capable to exert four major effects (Chen, 2001; Reznickova et al., 2011) surface cleaning, surface ablation or etching, surface cross-linking, and modification of the surface chemical structure, occurring both *in situ* or after subsequent exposure to the atmosphere. These effects depend on a presence of the active species in plasma (electrons, ions, radicals, photons) which interact with polymer surfaces and modify their chemical and physical properties. Ion irradiation is an established tool for modifying the chemical structure and physical properties of the polymers Pelagad et al, 1980; Chico et al., 2012). The ion beam irradiation technique has proven more effective in modifying polymer than other particle beam irradiation techniques because of its higher cross section for ionization and larger linear energy transfer (Drabik et al., 2007). Our aim of this work was intended to use plasma and ion beam currents produced from cold cathode ion source as a method for the morphology and wettability of semi crystalline poly ethylene terephtalate (PET) foils are treated and investigated.

EXPERIMENTAL OUTLINES

A schematic diagram of the cold cathode ion source and its associated electrical circuit is shown in Figure 1. It consists essentially of stainless steel anode cylinder with 30 mm length and 22 mm diameter connected with positive voltage power supply of +10 kV, cathode disc of diameter 22 mm and 2 mm thickness, and a semitransparent 50% as exit aperture. The extractor electrode connected to negative voltage power supply, Faraday cup placed at 30 mm distance from an exit aperture. PET sample put on faraday cup at distance 3 cm from the cylindrical cathode. A PET samples are immersed in acetone liquid and put it in ultrasonic apparatus to clean it. Cold cathode ion source was used to obtain the Argon plasma and ion beam and consequently irradiation PET surface using Argon plasma and ions. PET is polyester having a high melting point due to the presence of aromatic ring and has a very good mechanical strength. It is semi-crystalline in nature and is resistant to heat and moisture and virtually unattached by many chemicals. It has extensive use in textile fibers.

The working gas is admitted to the ion source through a hose fixed in a Perspex flange at the upper side of the anode. A complete vacuum system is used to evacuate the ion source chamber. It consists of stainless steel mercury diffusion pump of speed 270 l/s provided with electrical heater and backed by 450 l/min rotary fore-line vacuum pump. The rotary pump is used to evacuate the system to pressure of 10^{-2} to 10^{-3} mbar, while the mercury oil diffusion pump is used to evacuate the ion source vacuum chamber to the order of 10^{-5} mbar. A liquid nitrogen trap is fixed between the ion source chamber and the mercury oil diffusion pump in order to prevent the mercury vapor from entering the ion source chamber. The working gas is transmitted to the ion source from a gas cylinder through a needle valve to regulate the rate of gas flow. The plasma generation for this ion source is based on the ionization mechanism produced by primary electrons colliding with gas molecules due to a potential difference between the anode and the cathode. Therefore, high output ion beam current can be extracted axially in a direction normal to the discharge region. The anode is made of stainless steel material which is featured by high ionization coefficient and it is cylinder to improve the stability of the discharge. PET samples were put on Faraday cup at distance 3 cm from the anticathode. A PET samples are immersed in acetone liquid and put it in ultrasonic apparatus to clean it. Cold cathode ion source was used to obtain the plasma and Argon ion beams and consequently irradiation PET surface using plasma and Argon ions. PET is polyester having a high melting point due to the presence of aromatic ring and has a very good mechanical strength (Soliman et al., 2013). It is semi-crystalline in nature and is resistant to heat and moisture and virtually unattached by many chemicals. It has extensive use in textile fibers.

RESULTS AND DISCUSSION

In this study, the system is evacuated to about 3×10^{-5} mbar to remove the residual gases before the Argon gas injection in the ion source. The ion source apparatus was cleaned before introducing inside the vacuum system. It was polished, and washed by acetone. The polishing of the electrode parts should remove the irregular parts from their surfaces and the contamination due to the erode materials of the discharge. The plasma and the extracted Argon ion beam from the cold cathode ion source were used to irradiate Polyethylene terephthalate (PET). The sample considered in our investigations was PET (polyethylene terephthalate), provided by Goodfellow Company. The polymer samples, 50 µm thickness foils, were cut into 10×10 mm pieces, ultrasonically cleaned in alcohol to remove organic material and dried with hot air before treatment. The PET films are exposed to Argon plasma exposure process. We use plasma technique "reactive ion etching (RIE) system" with the Argon plasma parameters are the working pressure is 2×10^{-4} mbar and discharge voltage 900 volte, g = 180 gauss varied time exposure from 0 to 4 min and Argon ion beam for 0 to 4 h.

In the present work, discharge and output characteristics of this ion source using Argon plasma and Argon ion beams were done and this type of ion sources was used as a preparation tool of the surface of PET polymer substrate to be ready for coating or thin film deposition. Modifications in optical and surface properties of PET polymer induced by Ar plasma and Ar ion beam irradiation have been investigated in Atomic Energy Authority – Egypt), by:

1) FTIR spectra of the pristine and the irradiated samples were investigated using (FTIR-Beckman-4250) spectrophotometer in the range 400 cm^{-1} to 4000 cm^{-1} at National Center for Radiation Research and Technology (NCRRT), AEA, Cairo, Egypt. The irradiated PET films were exposed to atmosphere for a few days before the FTIR experiments were conducted.
2) SEM (Model, JEOL, Japan) at NCRRT, AEA, Cairo, Egypt, was used to investigate the surface morphology of the pristine and PET surfaces after bombarded by Argon plasma and Argon ion beam.

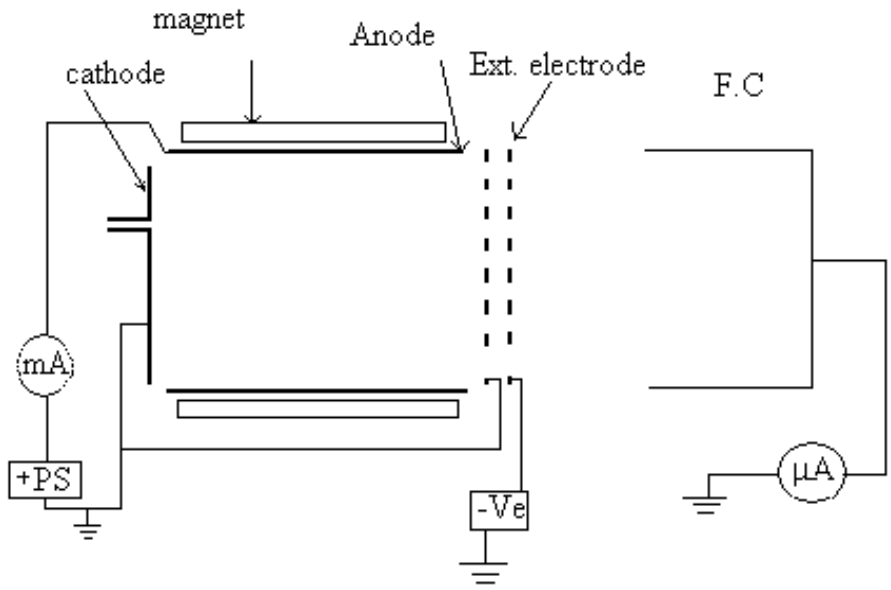

Figure 1. Experimental arrangement for irradiation of polymer samples using Ar plasma and Ar ion beam.

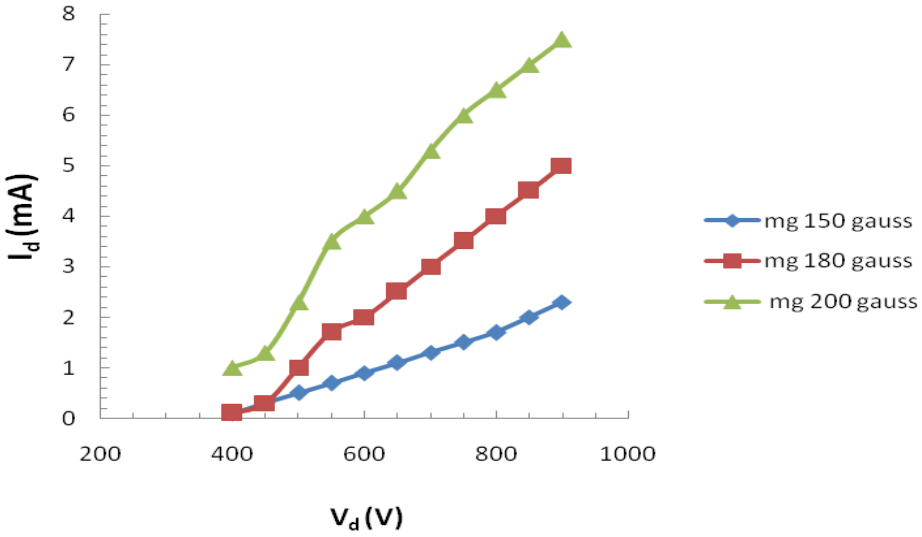

Figure 2. The relation between the electrical discharge current and the electrical discharge voltage with different magnetic field intensities.

3) The contact angle in a sessile drop method was measured by a contact angle meter (Cam Micro, Tantec). Each value of the contact angles was taken as an average from the five different samples fabricated under the same modification conditions. Surface free energy, that is, the sum of the polar force and the dispersion force, was calculated by measuring the contact angles of three different polar liquids (water and diiodomethane). From the measured contact angles, the polar forces and the dispersion forces were calculated using the Owen method (Soliman et al., 2013).

Ion source characteristics

Figure 2 shows the relation between the electrical discharge current, I_d, and the electrical discharge voltage, V_d, at pressures P = 2 × 10^{-4} mbar using Argon gas. It is clear that by increasing the discharge voltage, the discharge current increases at different magnetic field

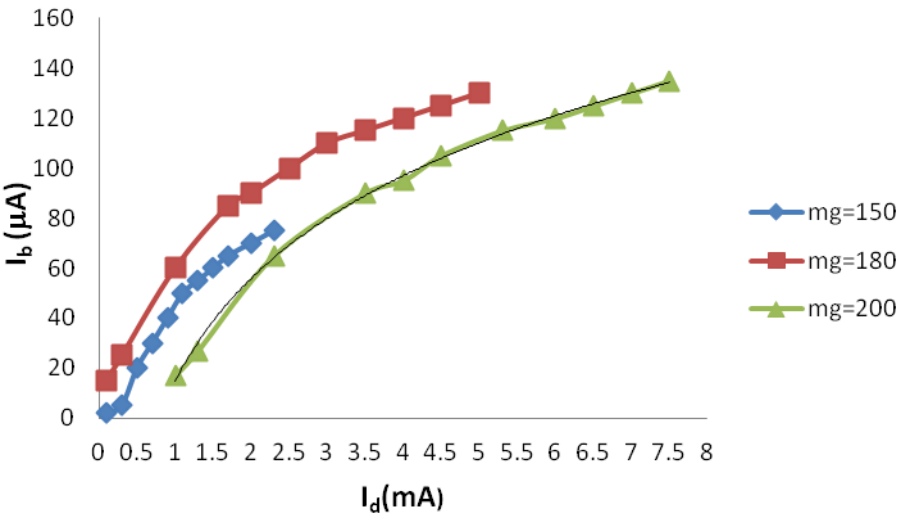

Figure 3. The relation between the electrical discharge current and the output ion beam current, with different magnetic field intensities.

intensities where the characteristic of such discharge is characterized by abnormal glow (Abdelrahman et al., 2008). This magnetic field is created an electromagnet coil wrapped around the cylindrical anode. Whereas, this magnetic field provides an increase of electron trajectories, hence, increasing the electron path which enhances the probability of ionization and then increase the discharge current. It was also found that an increase in magnetic field intensity was accompanied by an increase in the discharge current. This increase may be due to an increase in magnetic field vector parallel anode surface, and this leads to minimization in electron current in the anode region (Kotov 2004).

Figure 3 shows the relation between the electrical discharge current, I_d and the output ion beam current, I_b at 150, 180 and 200 gauss magnetic field intensities without extraction voltage. It could be seen that from this figure, maximum output ion beam current was obtained at magnetic field intensity of 180 gauss.

Figure 4 shows the relation between the electrical discharge current, I_d and the output ion beam current, I_b at 180 gauss magnetic field intensity with extraction voltage V_{ext} = - 600 V. It could be found from this figure that, an increase of the discharge current was accompanied by an increase of the output ion beam current at magnetic field intensity of 180 gauss and Argon gas pressure, $P_{Ar} = 2\times10^{-4}$ mbar.

Plasma and ion beam irradiation of polymers

The irradiation of all the polymer samples used in the present study were carried out by locally designed, a modified saddle field ion source at Egyptian Atomic Energy Authority, Egypt. The Ar ion beam irradiation was carried out in a vacuum chamber of 10^{-5} mbar, using a modified saddle field ion source. The ion fluence was estimated by time of irradiation and beam current as (Soliman et al., 2013):

$$I = Q/t = Dqe/t = \phi Aqe/t$$

Where I ion current (A), Q total charge, D: dose (ion fluence in ions / cm^2 × area (A) of irradiation in cm^2. and q is the charge state, e electron charge (1.6×10^{-19} C), finally t is the irradiation time in seconds.

FTIR spectral studies

FTIR spectroscopy has been found to be an important technique to understand the changes in the molecular bonds after irradiation. The changes have been observed from the relative increase or decrease in the intensity of the typical bands associated to the functional group present in the polymers. FTIR spectrum of pristine, Argon plasma and Argon ion beam irradiated PET are shown in Figure 5. By bombardment, the PET polymers by Argon plasma and ion beam were observed to decrease in the band intensities. It might be ascribed to the possible transient recrystallization due to Argon plasma and ion beam effect. The reduction in the intensity of the typical bands indicates some degradation of PET polymer by plasma and ion beam (Zhiyong et al., 2009). The infrared absorption spectra of the PET substrates in a wave number range of 2000 to 4000 cm^{-1} reveal the presence of an absorbance band at about case of Argon plasma than Argon ion beam.

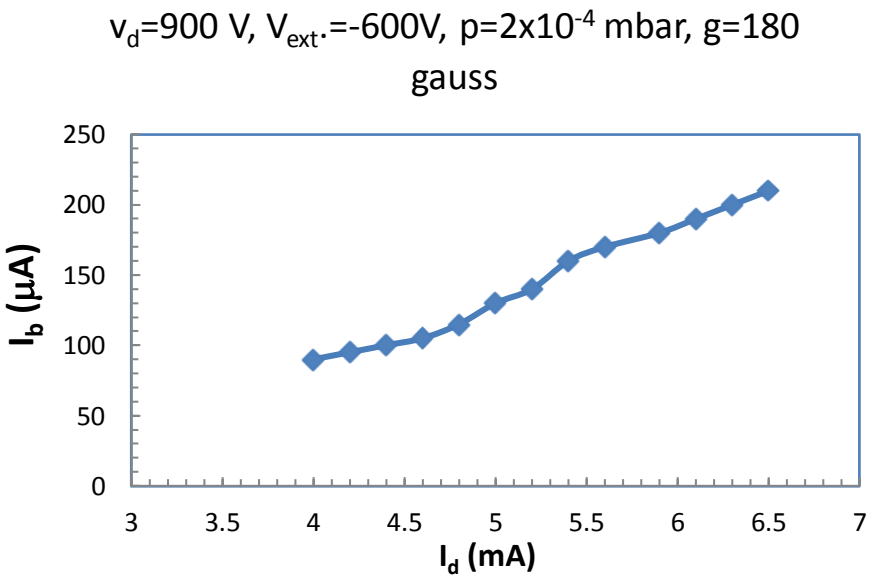

Figure 4. Output ion beam current versus discharge current using Argon gas at P = 2×10^{-4} mbar.

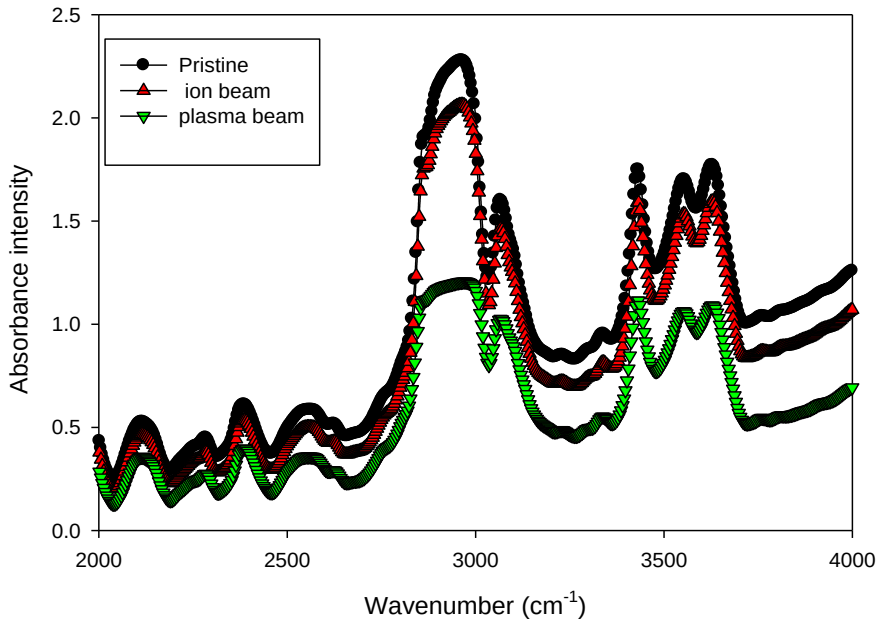

Figure 5. FTIR spectra of the pristine and irradiated PET films using Argon plasma and ion beams.

Scanning electron microscopy (SEM)

Polyethylene terephthalate (PET) film is transparent and the surface is smooth (Costa et al., 1997). The color of films gradually changes with irradiation from. The change in the color of polymer could be attributed to the formation of hydrogenous carbon clusters. The pristine sample showed rather relatively smooth surface as shown in Figure 6a. On the other hand, the SEM micrographs of irradiated samples by Argon ion beam display numerous small voids on the surface of the PET shown in Figure 6b. By using irradiated plasma, there was clear roughness on the surface of the irradiated samples and the resulting voids become large sized as

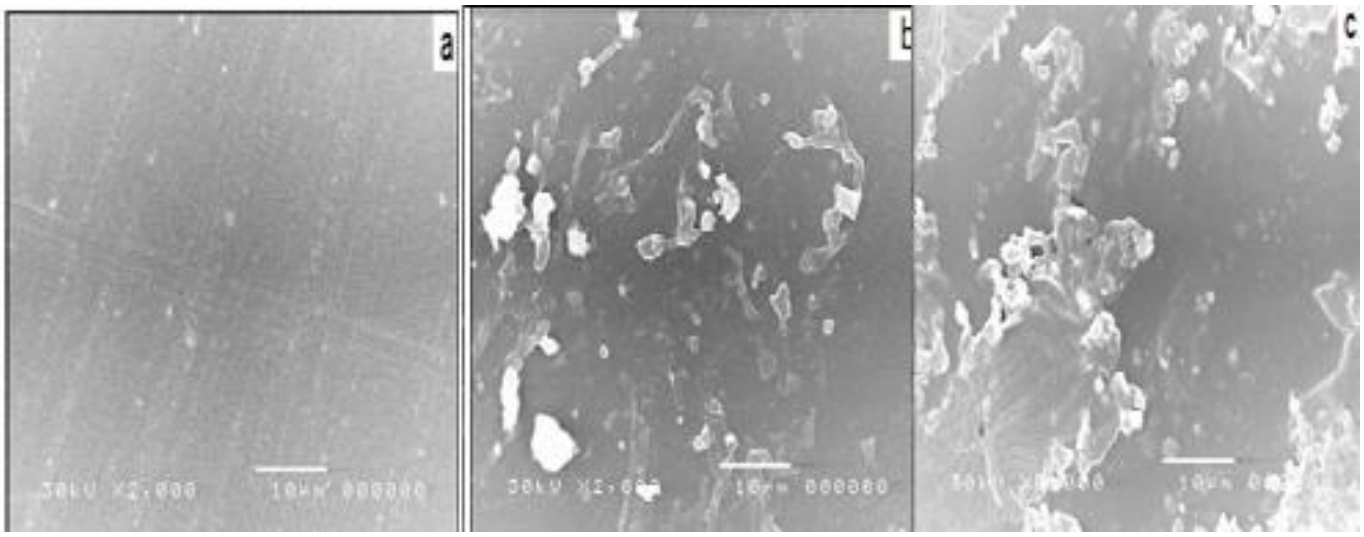

Figure 6. SEM micrographs for the pristine and irradiated PET by using Argon plasma and ion beams.

shown in Figure 6c. Bombardment of PET by Argon plasma is more efficient than Argon ion beam.

Surface wettability

Wettability and adhesion of polymers / films can be controlled by using surface modification techniques such as exposure to plasma, ion beams, flame, chemicals, enzymes etc. Wettability can also be regulated by changing chemical composition of the surface. In addition, surface roughness can be an important factor for enhancing the adhesion and wettability. Wettability is governed by molecular interaction of the outermost surface layer of a few angstrom units.

Contact angle is one from several independent methods that has been used to estimate solid surface tension (Liqing et al., 2009). Contact angle measurement is easily performed by establishing the tangent (angle) of a liquid drop with a solid surface.

$$\frac{y_l(1+\cos\theta)}{2\sqrt{y_l^d}} = \sqrt{y_s^d} + \sqrt{y_s^p}\cdot\sqrt{\frac{y_l^p}{y_l^d}} \qquad (1)$$

Equation 1 contains two unknowns' dispersive (γ_s^d) and polar (γ_s^p) surface energies of the solid (Soliman et al., 2013). To obtain these unknown parameters, one has to use contact angle measurements of at least two different liquids from Table 1.

The change in the contact angle on PET as a function of plasma expoure time and ion beam fluence are shown in Figure 7a and b, respectively. It can be noted that as the exposure time increases, the contact angle decreases. The water contact angle decreases from 75 to 2.9° in case of plasma and decreased to 44° by using ion beam as shown in Table 2. The change of contact angles for the irradiated polymers is due to the formation of hydrophilic groups rather than the change of surface roughness. Hydrophilic group formation is composed of a two-step process. The first one is the creation of free radicals on a polymer surface by plasma irradiation. In the second step, interaction between free radicals in polymer chains and oxygen atoms results in the formation of polar groups such as carboxyl, carbonyl, hydroxyl and ester groups (Fernando et al., 2007). Thus, the decrease of the contact angle as a function of exposure time is due to the formation of new hydrophilic groups and the oxidized layer on the surface of polymer (Costa et al., 1998).

Surface free energy

The change in the surface free energy of PET as function of Argon plasma exposure time (min) and ion beam fluency were observed in Figure 8a, b, respectively. The surface free energy increased from 35 to 75 and 62.6 mJ/m^2 by using Argon plasma and Argon ion beam, respectively. Also, one notes that the irradiations effectively increase the polar component and the dispersive component as shown in Table 3. Increasing the polar component in polymer is mainly due to the formation of polar and/or hydrophilic groups. From these results, the large decrease in contact angle can be attributed to the dominant increase of the polar component in the surface free energy of the modified polymers.

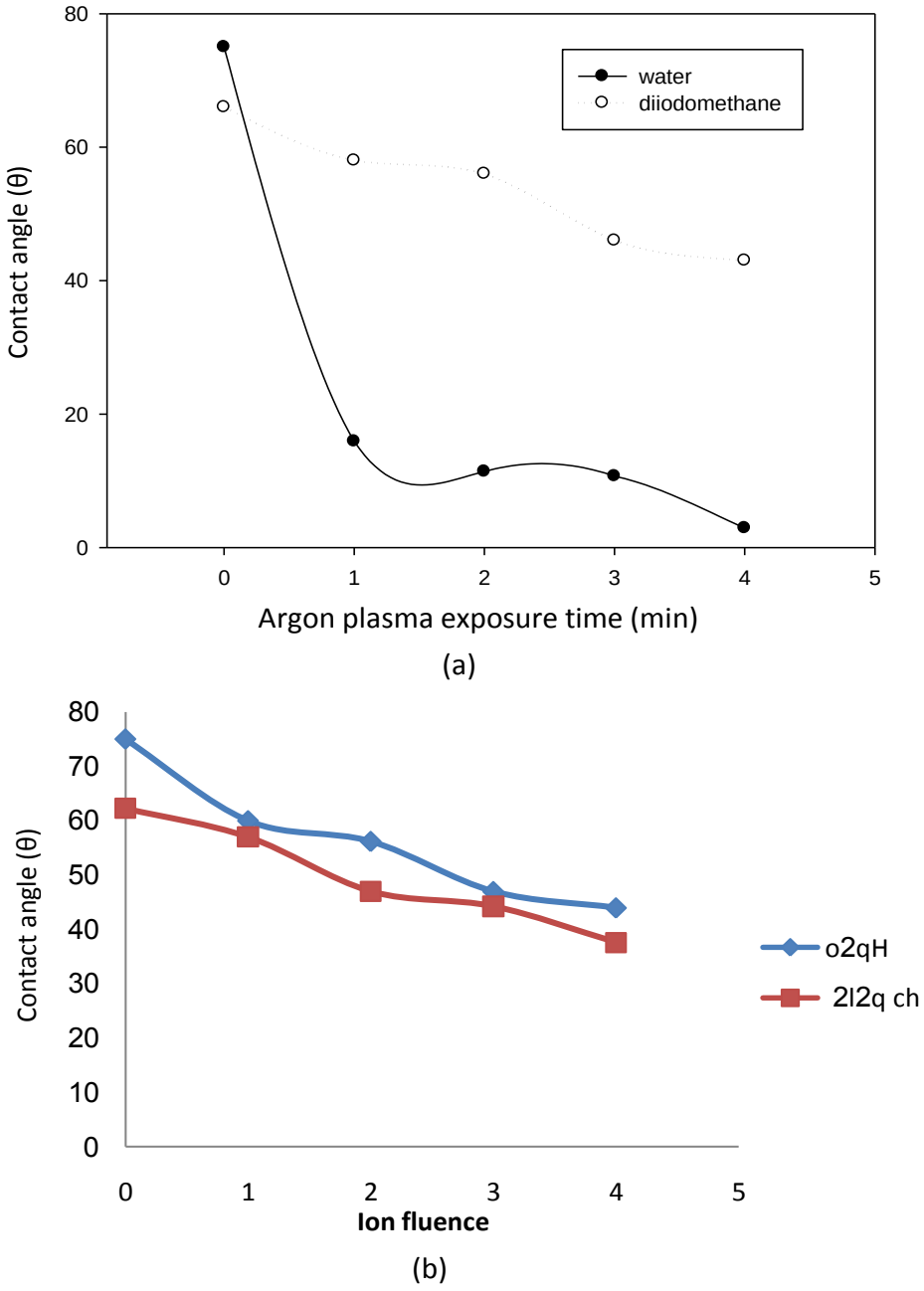

Figure 7. a) Change in the contact angle of PETas a function of Argon plasma exposure time; b) Change in the contact angle of PET as a function of Argon ion beam fluence.

Conclusions

In this work, it was concluded that, the characteristics of cold cathode ion source were studied with different operating parameters to get the optimum conditions for use in plasma and ion beam irradiation of some polymer materials. It could be found from this figure that, an increase of the discharge current was accompanied by an increase of the output ion beam current at magnetic field intensity of 180 gauss and Argon gas pressure, P_{Ar} = 2×10^{-4} mbar. Such results showed that this cold cathode ion source is quite suitable for impact processes, as it gives high discharge and ion beam currents with a wide beam diameter up to 2.2 cm. The effect of the Argon plasma and ion beam treatment on the surface properties of polyethylene terephtalate (PET) polymers was studied. The infrared absorption spectra of the PET substrates in a wave number range of 2000 to 4000 cm^{-1} reveal the presence of an absorbance band at about 2930 cm^{-1}. The intensity of bands is more reduction in case of

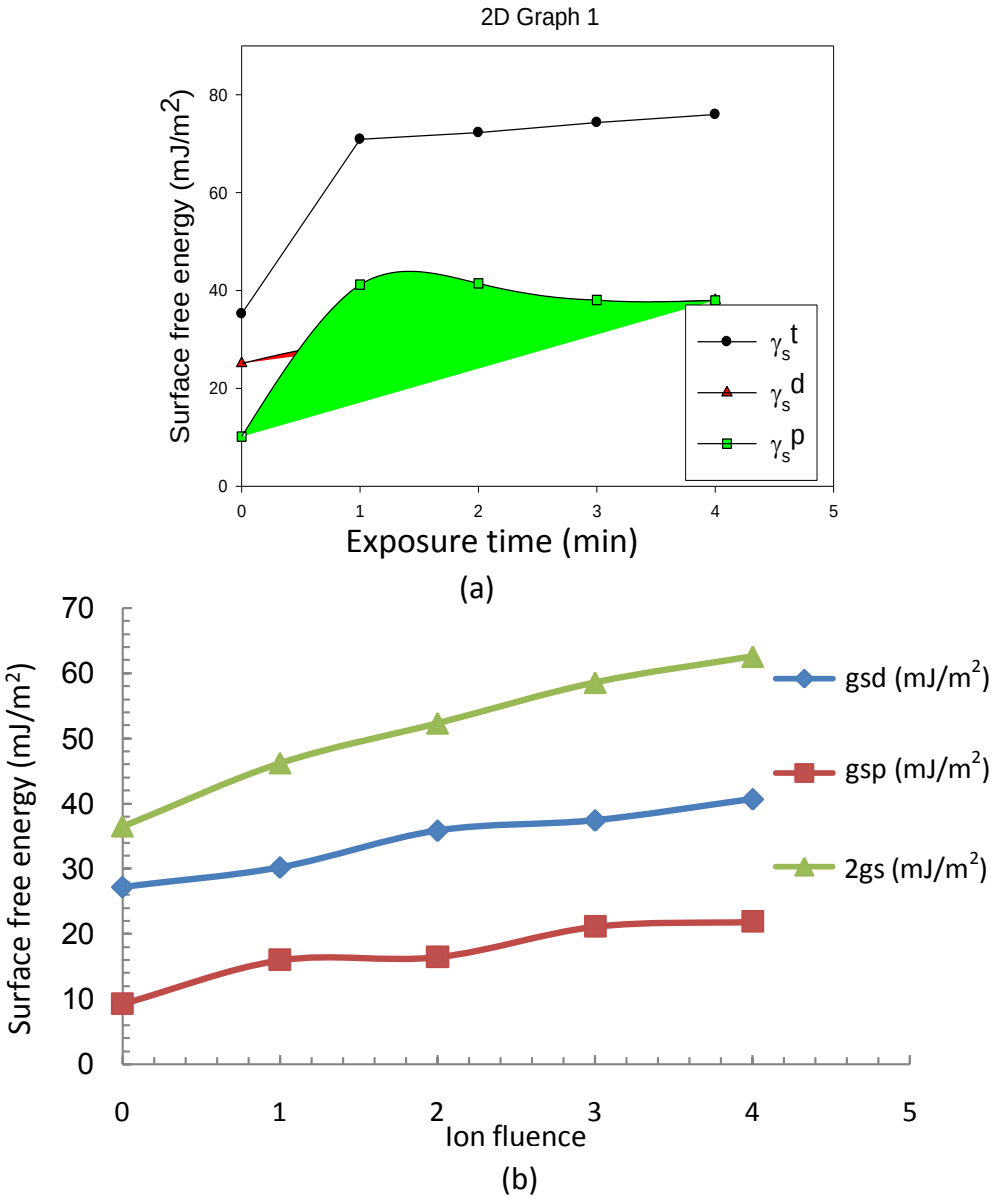

Figure 8. (a) Change in the surface free energy for PET as a function of Argon plasma exposure time; (b) Change in the surface free energy for PET as a function of Argon ion beam fluence.

Table 1. Surface free energy of the proposed liquids (Liqing et al., 2009).

Liquid	Surface free energy γ_l (Nm)	Polar component γ_l^p (Nm)	Dispersion component γ_l^d (Nm)
Water	72.1	52.2	19.9
Ch_2I_2	50.8	0	50.8

Argon plasma than Argon ion beam.

The SEM micrographs of irradiated samples by Argon ion beam display numerous small voids on the surface of the PET. By irradiated using plasma, the roughnesses clearly on the surface of the irradiated samples and the voids have large size. Bombardment of PET by Argon plasma is more efficient than Argon ion beam; the surface free energy increased from 35 to 75 and 62.6 mJ/m^2 by using Argon plasma and Argon ion beam, respectively. The large decrease in contact angle can be

Table 2. The contact angles (θ) for PET surface as a function of plasma exposure time and ion beam fluence.

Exposure time (min.)	θ_{H2o}	θ_{ch2l2}	Ion fluence	θ_{H2o}	θ_{ch2l2}
Pristine	75.00	66.00	0	75.00	66.00
1	15.90	58.00	$1x10^{-18}$	60	57
2	11.40	56.00	$2x10^{-18}$	56.5	47
3	10.70	46.00	$3x10^{-18}$	47	44.25
4	2.90	43.00	$4x10^{-18}$	44	37.625

Table 3. The dispersive surface free energy (γ_σ^δ) and the polar surface free energy (γ_σ^π) for PET surface as a function of plasma exposure time and ion beam fluency.

Exposure time (min)	γ_σ^δ (mJ/m^2)	γ_σ^π (mJ/m^2)	γ_σ (mJ/m^2)	Ion fluence	γ_σ^δ (mJ/m^2)	γ_σ^π (mJ/m^2)	γ_σ (mJ/m^2)
Pristine	25.10	10.15	35.25	0	25.10	10.15	35.25
1	29.70	41.22	70.92	1×10^{-18}	30.25	16	46.25
2	30.80	41.47	72.28	2×10^{-18}	35.88	16.48	52.36
3	36.26	38.07	74.33	3×10^{-18}	37.45	21.16	58.61
4	38.01	37.97	75.98	4×10^{-18}	40.70	21.90	62.61

attributed to the dominant increase of the polar component in the surface free energy of the modified polymers in Argon plasma than Argon ion beam.

Conflict of Interests

The author(s) have not declared any conflict of interests.

REFERENCES

AbdelRahman MM, Helal A, Moustafa OA and Abdel Salam FW (2008). High efficiency glow discharge ion source. J. Nucl. Radiat. Phys. 3(1):1-9.

Chen JR (2001). Low-temperature Plasma Chemistry and Application, Science Press, Beijing p. 1.

Cho S, Han S, Kim KH, Beag YW, Koh SK (2003).Surface modification of polymers by ion-assisted reaction. Thin Solid Films. 445:332-341. http://dx.doi.org/10.1016/S0040-6090(03)01176-3

Chico B, Martinez L, Perez FJ (2005). Nitrogen ion implantation on stainless steel: AFM study of surface modification. Appl. Surf. Sci. 243(1-4):409-414. http://dx.doi.org/10.1016/j.apsusc.2004.09.097

Costa L, Luda MP, Trossarelli L, Brach del Prever EM, Crova M, Gallinaro P (1998). In vivo UHMWPE biodegradation of retrieved prosthesis. Biomater. 19(15):1371-85. http://dx.doi.org/10.1016/S0142-9612(98)00013-1

Drabika M, Kousala J, Pihosha Y, Choukourova A, Biedermana H, Slavinskaa D, Mackovac A, Boldyrevac A, Pesickad J (2007). Composite SiOx/hydrocarbon plasma polymer films prepared by RF magnetron sputtering of SiO2 and polyimide. Vacuum. 81(7):920–927. http://dx.doi.org/10.1016/j.vacuum.2006.10.013

Ektessabi AM, Yamaguchi K (2000). XPS study of ion beam modified polyimide films. Thin Solid Films 377:621-625. http://dx.doi.org/10.1016/S0040-6090(00)01444-9

Fernando SS, Christensen PA, Egerton TA, White JR (2007). Carbon dioxide evolution and carbonyl group development during photodegradation of polyethylene and polypropylene. Polym. Degrad. Stabil. 92(12):2163-2172. http://dx.doi.org/10.1016/j.polymdegradstab.2007.01.032

Kotov DA (2004). Broad beam low-energy ion source for ion-beam assisted deposition and material processing. Rev. Sci. Instr. 75(5):1934-1936. http://dx.doi.org/10.1063/1.1702109

Liqing Ya, Jierong C, Yafei G, Zheng Z (2009). Surface modification of a biomedical polyethylene terephthalate (PET) by air plasma. Appl. Surf. Sci. 255(8):4446-4451. http://dx.doi.org/10.1016/j.apsusc.2008.11.048

Reznickova A, Kolska Z, Hnatowicz V, Stopka P, Svorcik V (2011). Comparison of glow Argon plasma-induced surface changes of thermoplastic polymers. Nucl. Instrum. Methods B. 269(2):83-88. http://dx.doi.org/10.1016/j.nimb.2010.11.018

Pelagad SME, Singh NL, Qureshi A, Rane RS, Mukherjee S, Deshpande UP, Ganesan V, Shripathi T (2012). Investigation of surface properties of Ar-plasma treated polyethylene terephthalate (PET) films. Nucl. Instrum. Methods B. 289:34-38. http://dx.doi.org/10.1016/j.nimb.2012.08.010

Soliman BA, Abdel Rahman MM and Abdelsalam FW (2013). Irradiation effect on PET surface using low energy Argon ion beam. J. Nucl. Mater. 432(1-3):444-449. http://dx.doi.org/10.1016/j.jnucmat.2012.08.006

Zhiyong Z, Changlong L, Youmei S, Jie L, Yuhua T, Yucfan J, Junli D (2002). Modification of polyethylene terephthalate under high-energy heavy ion irradiation. Nucl. Instrum. Methods Phys. Res. B. 191(1-4):723-727. http://dx.doi.org/10.1016/S0168-583X(02)00641-9

Journal of
Engineering and Technology Research
OPEN ACCESS